Environ. Sci. Technol. **2007**, *41,* 1889−1895

Mercury Stable Isotope Fractionation during Reduction of Hg(II) to Hg(0) by Mercury Resistant Microorganisms

K. KRITEE,*,† JOEL D. BLUM,‡ MARCUS W. JOHNSON,‡ BRIDGET A. BERGQUIST,‡ AND TAMAR BARKAY†

Rutgers University, 76 Lipman Drive, New Jersey 08901, and University of Michigan, 1100 N. University Avenue, Michigan 48109

Mercury (Hg) undergoes systematic stable isotopic fractionation; therefore, isotopic signatures of Hg may provide a new tool to track sources, sinks, and dominant chemical transformation pathways of Hg in the environment. We investigated the isotopic fractionation of Hg by Hg(II) resistant (Hg^R) bacteria expressing the mercuric reductase (MerA) enzyme. The isotopic composition of both the reactant Hg(II) added to the growth medium and volatilized product (Hg(0)) was measured using cold vapor generation and multiple collector inductively coupled plasma mass spectrometry. We found that exponentially dividing pure cultures of a gram negative strain *Escherichia coli* JM109/pPB117 grown with abundant electron donor and high Hg(II) concentrations at 37, 30, and 22 °C, and a natural microbial consortium incubated in natural site water at 30 °C after enrichment of Hg^R microbes, preferentially reduced the lighter isotopes of Hg. In all cases, Hg underwent Rayleigh fractionation with the best estimates of $\alpha_{202/198}$ values ranging from 1.0013 to 1.0020. In the cultures grown at 37 °C, below a certain threshold Hg(II) concentration, the extent of fractionation decreased progressively. This study demonstrates mass-dependent kinetic fractionation of Hg and could lead to development of a new stable isotopic approach to the study of Hg biogeochemical cycling in the environment.

Introduction

Mercury (Hg) is often cited in fish consumption advisories across the world due to the extreme neurotoxicity of its methylated forms. Because Hg is globally distributed by atmospheric transport as Hg(0) (*1*), a differentiation between local vs global and natural vs anthropogenic sources of Hg(0) is critical. Moreover, since Hg enters the environment mostly in its inorganic form and transformations within the environment determine its toxicity, it is important to determine which transformations are dominant in a given ecosystem (*2*). Methods that provide insight into the sources, redox cycling, and other chemical transformations of Hg in ecosystems are, therefore, needed to better understand Hg bioavailability, the mechanisms for production and degradation of methylated Hg compounds, and the resultant toxicity of Hg.

Stable isotope ratios of many light elements (i.e., C, N, O, S) have proven useful as proxies for determining sources, sinks, and dominant transformation pathways of nutrients and toxic substances in present and paleo environments (*3*). The measurement and application of stable isotope fractionation of heavier elements such as Fe, Cr, Se, Cu, and Zn has recently become possible with the advent of new instrumentation and analytical techniques (*4*−*6*). Because Hg has seven stable isotopes (^{196}Hg, ^{198}Hg, ^{199}Hg, ^{200}Hg, ^{201}Hg, ^{202}Hg, and ^{204}Hg) with a relative mass difference of 4%, and it undergoes redox transformations involving compounds with a high degree of covalent character, measurable stable isotope fractionation of Hg could occur during its transformations in the environment. Indeed, significant Hg isotope variations in natural samples from hydrothermal ores (*7*−*8*), sediment cores (9-*10*), and fish tissues (*11*) have recently been reported, but the causes of the observed fractionations have not yet been explored. This study reports one process that can lead to Hg isotopic fractionation seen in natural samples.

Development of any new stable isotope proxy for addressing complex biogeochemical phenomena requires the determination of fractionation factors for individual biotic and abiotic transformations that occur in the environment. For Hg, one such transformation is the reduction of Hg(II) to Hg(0), which is an important pathway in its biogeochemistry as it adds to the pool of Hg(0) available for atmospheric global transport (*12*), and also reduces the amount of Hg(II) available for MeHg synthesis (*13*−*14*). We hypothesized that bacteria expressing the enzyme mercuric reductase (MerA), an enzyme found in a broad range of Hg-resistant (Hg^R) bacteria from diverse environments, would lead to measurable preferential uptake and reduction of lighter isotopes of Hg and demonstrate kinetic fractionation. MerA is part of an elaborate resistance mechanism that is mediated by the mercury resistance (*mer*) operon. This Hg(II) inducible operon has evolved to protect microorganisms from the toxicity of Hg(II) by removing it from their environment in the form of Hg(0), and mediates the most efficient biological reduction of Hg(II). At their optimum growth conditions, actively growing MerA expressing bacterial cultures (~10^5−10^6 cells/mL) can reduce 99% of a 20 μg Hg(II) per 1 g of growth medium in less than an hour. In natural uncontaminated environments between 1 and 10%, and in Hg contaminated environments up to 50%, of the culturable microbes are Hg^R and likely have a functional MerA (*15*).

The extent of stable isotope fractionation during microbial transformations can change with the bacterial species involved, the quantity and quality of nutrients, and other environmental factors including pH, temperature, and redox conditions that can change reaction pathways or rate-limiting steps (*5*, *16*) and the degree of reaction completion (*17*). Therefore, before isotope ratios can be interpreted within the complexity of environmental samples, controlled laboratory experiments are required to assess the effect of individual variables on the extent and expression of isotopic fractionation. Here, we performed high precision Hg stable isotope measurements by cold vapor generation coupled with multiple collector inductively coupled plasma mass spectrometry (MC-ICPMS) to show fractionation of Hg isotopes during the reduction of Hg(II) by a pure culture at differing temperatures and by natural microbial communities.

* Corresponding author phone: 1-732-932-9763 x334; fax: 1-732-932-8965; e-mail: kritee@eden.rutgers.edu.
† Rutgers University.
‡ University of Michigan.

10.1021/es062019t CCC: $37.00
Published on Web 02/09/2007

Materials and Methods

All experiments were performed in an autoclaved glass or Teflon apparatus that was cleaned by soaking in either 8N HNO_3 or 10% BrCl overnight followed by rinsing five times in 18 MΩ deionized water. All inoculated and uninoculated control experiments were carried out in the dark to isolate biological reduction from possible photochemical reduction pathways. Details of the reagents used, the experimental setup, sample collection and preservation, Hg concentration and isotopic composition analyses, mathematical treatment of data, and approximations employed are described below (also see the Supporting Information).

Mercury Reduction by Hg^R Gram Negative Pure Culture. *Escherichia coli* strain JM109 carrying the mercury resistance plasmid pPB117 (hereafter *E. coli* JM109/pPB117) was used in Hg(II) reduction experiments. The plasmid pPB117 originated in the soil bacterium *Pseudomonas stutzeri* (*18*). *E. coli* JM109/pPB117 was grown in M9 defined medium (*19*) supplemented with 1% pyruvate at 37, 30, or 22 °C. This medium was used to achieve very slow bacterial growth rates of about 1.5 h per generation at 37 °C (*20*) (typical growth rate in rich media is ∼20 min per generation) and consequently decrease the rate of Hg(II) reduction. Bacterial cultures grown overnight at 37 °C were diluted to an optical density (OD) of 0.05 at 660 nm and incubated at the selected growth temperature in the presence of 600 ng Hg(II) per g of the growth medium until the OD increased to 0.2. About 30 min before using it as an inoculum, another dose of 600 ng/g Hg(II) was added to induce *merA* (*15*). Cultures were then diluted 1:1000, yielding a cell density of $\sim 10^5$ colony forming units per mL (CFU/mL), into a Pyrex glass reactor wrapped with aluminum foil (100 or 1000 mL) connected to traps with a Hg(0) trapping solution (0.05M $KMnO_4$ [Hg grade] and 5% H_2SO_4 [Fisher Trace Metal Grade]) via a soda lime drying tube. NIST SRM (Standard Reference Material) 3133 available as $Hg[NO_3]_2$ (with a certified Hg concentration of 10.00 ± 0.02 mg/g) was added to the reactor to reach a final concentration of 600 ng/g, and the Hg(0) volatilized during the growth was purged into the trapping solution by sparging the culture solution with Hg-free air at a rate of 35 mL/min. The cells remained in exponential growth phase throughout the length of our experiments. Experiments with *E. coli* JM109/pPB117 were done multiple times in 100 mL reactors at all three growth temperatures. In addition, experiments were done twice at 37 °C and once at 30 °C in a larger 1 L reactor that allowed for sample withdrawal from the reactor and isotopic analysis of the remaining reactant [Hg(II)], as well as the analysis of the collected product [Hg(0)] as a function of time.

Mercury Reduction by Hg^R and Hg(II) "Sensitive" (Hg^S) Natural Microbial Communities. Water samples from a freshwater pond, Passion Puddle (on the grounds of Rutgers University, New Brunswick), with no known point sources of mercury, were pre-exposed to $HgCl_2$ to adapt the indigenous microbial community to Hg(II) and enrich for Hg^R microbes (*21*). Mercuric chloride was added to 300 mL of site water to achieve a final concentration of 225 ng/g and incubated at 30 °C. After 4 days, cells were harvested by centrifugation (at 4300 × g for 25 min in a Sorvall RC-5B Superspeed centrifuge) and resuspended in 300 mL of filtered (0.2 μm pore size Millipore Durapore membrane filter) site water containing 225 ng/g Hg(II) (NIST 3133 standard) in a 1 L reactor wrapped with aluminum foil. The reactor solution was constantly sparged with Hg free air.

The acclimation to Hg(II) was followed by counting the number of total heterotrophic and Hg^R colonies during the 4 days of the pre-exposure period. Water samples withdrawn from the reactor were diluted serially in 0.85% NaCl and plated on modified LB medium (3 g yeast extract, 5 g NaCl, 6 g trypton and 15 g agar in 1 L water) with and without 20 μM (4 μg/g) Hg(II) in petri plates. Plates were incubated for 3 days at room temperature, after which the number of visible colonies were counted and CFU/mL of total and Hg^R microorganisms present were calculated. Another experiment with the unadapted natural Hg^S microbial community consisted of an unexposed Passion Puddle water sample in a 1 L reactor supplemented with 25 ng/g Hg(II). A dark abiotic control experiment was performed by purging filter-sterilized (0.2 μm filter) Passion Puddle water sample containing 225 ng/g Hg(II).

Sample Collection. To determine the change in isotopic composition of the product Hg(0) as a function of the fraction of added Hg(II) that remained in the reactor (f), traps were replaced periodically to collect the volatilized Hg(0). For experiments done with *E. coli* JM109/pPB117 at 37 °C, traps were replaced every ∼35 min for a period of ∼300 min, for those at 30 °C, traps were replaced every ∼60 min for a period of ∼550 min, for those done at 22 °C, traps were replaced every ∼90 min for a period of ∼800 min The isotopic composition of the trap sample collected does not represent the isotopic composition of instantaneous product but rather a time integrated product (see below).

To determine the isotopic composition of the reactant Hg(II) in the reactor as a function of "f", ∼20 mL samples were withdrawn from the 1 L reactor at the same time that the traps were replaced and were preserved by the addition of 0.2% HCl (w/w) and 10% BrCl (w/w). For the experiment with natural microbial communities, reactor samples were taken every 10-12 h for a period of 50−60 h.

Mercury Concentration and Stable Isotopic Composition Analysis. Concentrations of Hg(II) in the reactor and trap solutions were measured using atomic absorption spectroscopy (AAS; Hydra AA, Leeman Labs) at Rutgers University as soon as the experiments were completed. Preserved reactor and trap samples were analyzed for their Hg isotopic composition using a Nu Instruments MC-ICPMS at the University of Michigan. Samples were introduced into the mass spectrometer using cold vapor generation with Sn(II) reduction, which ensures complete reduction of Hg(II) in the sample and does not cause any fractionation (*22*). Instrumental mass bias was corrected using both a thallium (NIST 997) internal standard and standard-sample bracketing with the NIST SRM 3133 standard (*22, 23*). The Tl internal spike was added to the Hg vapor after cold vapor generation via an Aridus desolvating nebulizer (*23*). Prior to introduction to the cold vapor generator and MC-ICPMS, samples were partially reduced with hydroxylamine hydrochloride to reduce excess $KMnO_4$ (in trap samples) or excess BrCl (in reactor samples) and diluted to a final concentration of 35 ng/g or less. About 7 mL of solution was used for each individual analysis. Sample concentrations were matched within 10% to the bracketing standard (NIST SRM 3133), and the matrix of the bracketing standard was matched to the samples (either $KMnO_4$ or BrCl). In addition, on-peak zero corrections were applied to all masses and the ^{204}Pb interference on ^{204}Hg was corrected by monitoring ^{206}Pb. All procedural blanks were routinely analyzed for Hg. For a typical 7 mL sample, reactor and trapping solution blanks had Hg concentrations of <0.75 ng/g and <0.15 ng/g, respectively, which were too low to be accurately analyzed for isotopic composition. Mercury isotopes are reported here in delta notation, in units of per mil (‰), referenced to a Hg standard (NIST 3133) and unless otherwise indicated, $\delta^{202}Hg$ refers to $\delta^{202}Hg/^{198}Hg$ and is calculated as follows:

$$\delta^{202}\mathrm{Hg} = \left(\frac{(^{202}\mathrm{Hg}/^{198}\mathrm{Hg})_{\mathrm{sample}}}{(^{202}\mathrm{Hg}/^{198}\mathrm{Hg})_{\mathrm{NIST}}} - 1 \right) \times 1000$$

To ensure that the measured fractionation observed was mass dependent and that the isotope ratios measured were free of interferences, multiple isotope ratios (i.e., $^{200}Hg/^{198}Hg$, $^{201}Hg/^{198}Hg$, $^{202}Hg/^{198}Hg$, and $^{204}Hg/^{198}Hg$) were measured.

The typical internal (instrumental) precision for natural samples was better than ±0.003% (RSE) for all measured ratios. The uncertainty (external precision) for $\delta^{202}Hg$ in this paper has been estimated in two different ways: (1) the 2SD of repeated analyses of our in-house Almaden Standard prepared in the same matrix as the samples [$\delta^{202}Hg = -0.54 \pm 0.09$‰ (2SD, BrCl matrix, $n = 14$) and -0.58 ± 0.19‰ (2SD, $KMnO_4$ matrix, $n = 13$)], and (2) the 2SE of replicate analyses of each sample. To be conservative, error bars on Rayleigh plots and uncertainties used during linear regression of data (*25*) are based on the larger of these two values for each sample.

Calculations. The kinetic fractionation factor ($\alpha = (^{202}Hg/^{198}Hg)_{reactant}/(^{202}Hg/^{198}Hg)_{product}$) was determined from the results of our experiments using the following two forms of the Rayleigh distillation equation as described by Hoefs (*17*) and Scott et al. (*24*). These equations were used to infer the value of α using the relative isotope ratio data from the reactor (containing the liquid phase) and traps (containing samples corresponding to the time integrated product in the vapor phase), respectively.

$$\ln(R_{Li}/R_{Lo}) = ((1/\alpha) - 1)\ln(f) \quad (1)$$

$$\ln(R_{Vi}/R_{Lo}) = ((1/\alpha) - 1)\ln(f) + \ln(1/\alpha) \quad (2)$$

where R = relative isotope ratio $(^{202}Hg/^{198}Hg)_{sample}/(^{202}Hg/^{198}Hg)_{NIST\ 3133}$; V = vapor phase [Hg(0) in trap]; L = liquid phase [Hg(II) in the reactor]; $\alpha = (^{202}Hg/^{198}Hg)_{instantaneuos\ reactant}/(^{202}Hg/^{198}Hg)_{instantaneous\ product}$; f = fraction of added Hg(II) remaining $\{f^R = [Hg]_{Li}/[Hg]_{Lo}$ and $f^T = ([Hg]_{Lo} - \Sigma[Hg]_{Vi})/[Hg]_{Lo}\}$; 0 = 0 min; i = i minutes; [Hg] = total amount of mercury (ng).

Both the slope [$(1/\alpha) - 1$] of the linear Rayleigh plots for eq 1 and 2 and the intercept [$\ln(1/\alpha)$] of the plot for eq 2 were used to calculate the value of $\alpha_{202/198}$. Linear regressions were carried out by the York method (*25*) in which each data point is weighted according to its uncertainty. In the absence of replicate analyses (for 100 mL reactor experiments), 0.09 and 0.19‰ were used as uncertainties for reactor and trap samples, respectively (see uncertainty discussion above).

Best Estimates of Alpha Value. An $\alpha_{202/198}$ value based on the reactor isotope and concentration data is considered the best estimate of $\alpha_{202/198}$ value for that individual experiment. This is because reactor isotope data give the true instantaneous isotopic composition of the reactor at any given time (R_{Li} in eq 1 above), calculation of "f^R" does not involve any estimations, and the reproducibility (external precision) for the reactor samples (BrCl matrix) is better than for trap samples ($KMnO_4$ matrix).

Approximation Used to Calculate f^T. For the trap samples, an effective f^T was calculated as the average of f before and after the interval of time during which a particular trap accumulated the product Hg(0) because the isotopic composition of the traps represents a time-integrated product rather than the true instantaneous product composition (R_{Vi} in eq 2 above). Moreover, values of f^R calculated from reactor Hg concentration data are considered more reliable than f^T from the trap data (see the Supporting Information), and whenever possible (for all the experiments done using 1 L reactor), the values of averaged f^R were used in preference to averaged f^T as the effective f for traps (see above).

Results and Discussion

In all experiments, the trapped Hg(0) had a lower $\delta^{202}Hg$, i.e., was isotopically lighter, than the reactant Hg(II) (e.g., Figure 1). Both the product Hg(0) and reactant Hg(II) followed mass dependent (Figure 2) Rayleigh fractionation (Figures S1−S4, Supporting Information) as the experiments progressed, i.e., the Hg became isotopically heavier with the increasing extent of completion of the reaction.

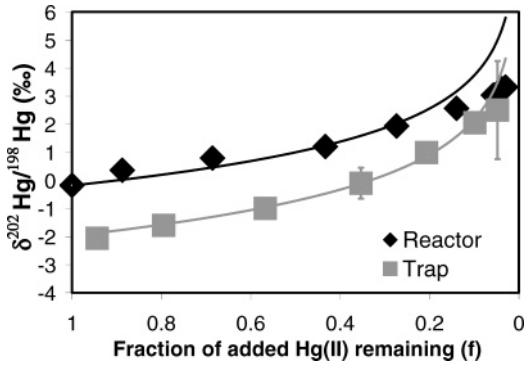

FIGURE 1. The isotope data for the experiment with *E. coli* JM109/pPB117 at 37 °C in a 1 L reactor plotted as $\delta^{202}Hg$ vs f. Error bars on the *y*-axis are based on the larger of two values (2SE of the isotopic analysis of n replicates of the sample or the 2SD of repeated analyses of in-house standard) and are, in most cases, hidden because they are smaller than the size of the symbols. Curves represent the predicted isotopic composition of the reactor and trap samples corresponding to $\alpha_{202/198}$ values of 1.0016 and 1.0020, respectively. A significant progressive suppression in isotope fractionation occurs below f < 0.3 (180 ng/g of Hg(II) remaining in the reactor).

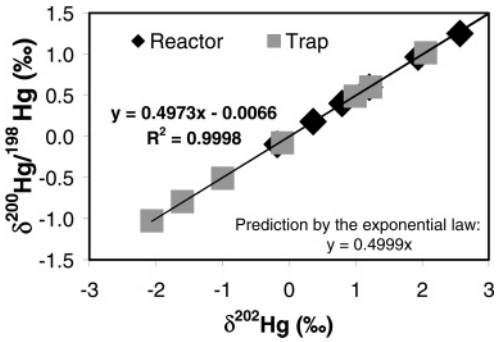

FIGURE 2. Mass dependence of fractionation. $\delta^{200}Hg/^{198}Hg$ vs $\delta^{202}Hg/^{198}Hg$ for the reactor and trap samples from an experiment done in 1 L reactor with *E. coli* JM109/pPB117 grown at 37 °C. The slope of the line agrees well with the slope predicted by mass dependent fractionation (*4*).

Table 1 summarizes the estimates of the fractionation factors ($\alpha = (^{202}Hg/^{198}Hg)_{reactant}/(^{202}Hg/^{198}Hg)_{product}$) based on the isotopic composition of the reactant Hg(II) remaining in the reactor and Hg(0) trapped in successive traps in these experiments, as modeled with the Rayleigh fractionation equation. The isotopic compositions of the reactant Hg(II) and product Hg(0) formed during microbial reduction (Tables S1−S4) and the Rayleigh plots (Figure S1−S4) are provided in the Supporting Information.

We discuss below the results of individual experiments in light of the well understood Hg(II) uptake and reduction mechanism in gram negative Hg^R bacteria (*15*, *26*). MerA mediated Hg(II) reduction is a complex process that includes diffusion through outer membrane, active transport (by MerT and MerP) across the periplasm and the inner membrane and interactions with thiol compounds (*15*). Thus, we suggest that, similar to the model that explains net sulfur fractionation during sulfate reduction by sulfate reducing bacteria (SRB) (*16*, *27*), the Hg fractionation observed will be the net effect of the fractionation at all of the individual steps before, and including, the rate-limiting step. It is important to note,

TABLE 1. Summary of $\alpha_{202/198}$ Values Obtained from Linear Regression of Isotope Data from All Experiments

conditions		based on reactor (eq. 1)[a]				based on trap (eq. 2)[a]						
temperature	reactor size	slope		2 SD	N[b]	slope		2 SD	intercept		2 SD	N[b]
pure culture: *E. coli* JM109/pPB117												
37 °C	1 L	1.0016	±	0.0005	5	1.0020	±	0.0002	1.0020	±	0.0002	5
	1 L	1.0014	±	0.0001	5	1.0017	±	0.0002	1.0020	±	0.0002	5
	100 mL	NA[c]			2	1.0020	±	0.0006	1.0020	±	0.0004	5
30 °C	1 L	1.0017	±	0.0003	10	1.0023	±	0.0002	1.0020	±	0.0001	9
22 °C	100 mL	1.0018	±	0.0004	2	1.0026	±	0.0014	1.0019	±	0.0004	6
	100 mL	1.0020	±	0.0002	2	1.0032	±	0.0009	1.0028	±	0.0005	10
natural microbial consortium												
adapted Hg(II) resistant	1 L	1.0013	±	0.0004	6							
unadapted Hg(II) sensitive	1 L	1.0004	±	0.0002	4							

[a] Refer to Materials and Methods section. [b] *N* is the number of data points used for regression (see Materials and Methods section for details). [c] Not applicable; one of the two data points available corresponds to $f = 0.08$.

however, that the reduction of Hg(II) is an energy-requiring detoxification mechanism and, therefore, is fundamentally different from the dissimilatory reduction of sulfate where SRB depend on sulfate for their growth (*16*) (or microbial reduction of terminal electron acceptors like nitrate (*3*), Se(VI) (*5*) and Fe(III) (*6*)).

Fractionation of Hg by *E. coli* JM109/pPB117 at its Optimum Growth Temperature. Repeat experiments with *E. coli* JM109/pPB117 were performed at its optimal growth temperature (37 °C) (Figure 1, Table S1, Figure S1, excluding data with f < 0.3, see discussion on the suppression of fractionation below) in either 100 mL or 1 L reactors. All experiments yielded similar or overlapping values of fractionation factors (based on the isotopic composition of either the Hg(II) that remained in the reactors or the Hg(0) in the successive traps) with the $\alpha_{202/198}$ values (Table 1) ranging from 1.0014 to 1.0020, demonstrating that the $\alpha_{202/198}$ values are reproducible regardless of reactor size.

Dark abiotic controls volatilized only 1.2% or less of the added Hg(II) in the reactor, and the δ^{202}Hg of the reactor did not change over the length of the experiments (0.05 ± 0.05‰). Thus, the small amount of Hg(II) that was reduced abiotically in the growth medium is unlikely to have had a significant effect on the observed biological reduction in our experimental setup. Purging of Hg(0) formed after abiotic reduction of Hg(II) by addition of $SnCl_2$ did not cause any fractionation (*22*) demonstrating that the fractionation observed in the biological reduction experiments was due to biological uptake and/or reduction of Hg(II) rather than fractionation during purging and transport of Hg(0) between the reactor and trap.

Concentration Dependent Suppression of Hg Fractionation. For the two pure culture experiments done at 37 °C in a 1L reactor (Table S1), we observed that when the fraction of added Hg(II) remaining in the reactor (f) fell below 0.3 (<180 ng/g), there was a progressive suppression in the amount of fractionation compared to the prediction of the Rayleigh model (Figure 1). Because all bacterial cells reducing Hg(II) were in the exponential growth phase (see methods) and there was an ample supply of nutrients in the bacterial growth medium throughout the length of the experiments, the suppression in fractionation was unlikely to have been due to changes in the bacterial growth phase or nutrient limitation. Moreover, since this suppression was not observed for experiments done at 30 and 22 °C (see Rayleigh plots in the Supporting Information), where f was always >0.3 (with the exception of one point; see Table S2) due to a slower growth rate of *E. coli*, this may be due to reactant [Hg(II)] limitation, as has been observed for some other stable isotope systems. There is considerable evidence that Hg(II) uptake is the rate-limiting step in the MerA mediated reduction of Hg(II) (*26* and references therein). For sulfur, it is thought that at low sulfate concentrations (<1 mM) sulfate exchange across the cell membrane is rate limiting, leading to lesser exchange of sulfate back out of the SRB and suppression in apparent sulfur isotope fractionation (*16*). We do not fully understand why there is drastic suppression in fractionation only after the Hg(II) concentration falls below 180 ng/g in the reactor. Nevertheless, we suggest that as the experiments progressed, the concentration and availability of the Hg(II) in the reactor decreased to the point where the molar ratio of reactant Hg(II) to "activated" Mer proteins became so low that it led to uptake and reduction of all the toxic Hg(II) in the cell's environment, diminishing the extent of fractionation. It is also plausible that as the cell density inside the reactor increased, the increasing amount of cell exudates sorbed Hg, further limiting the bioavailability of Hg(II) for uptake and reduction (*28*).

Effect of Growth Temperature on Hg Fractionation. The effect of growth temperature on the extent of isotopic fractionation by strain *E. coli* JM109/pPB117 was tested by incubating the reactor at 30 and 22 °C. A decrease in growth temperature from 37 to 30 °C increased the generation time of the bacterium from 90 to 195 min, decreasing the rate of Hg(0) volatilization and necessitating a doubling of the time interval between two consecutive sampling points relative to that at 37 °C (Table S2). Nevertheless, both the product Hg(0) and reactant Hg(II) followed Rayleigh fractionation (Figure S2), and the fractionation factors ($\alpha_{202/198}$) obtained were similar in range to those obtained for experiments at 37 °C (Table 1). When *E. coli* JM109/pPB117 was grown at 22 °C, the generation time of the bacterium increased to 300 min or more (Table S3, Figure S3), and the $\alpha_{202/198}$ values obtained using the reactor data are similar to those obtained at higher temperatures. The trap data from experiments done at 22 °C implied slightly higher values of $\alpha_{202/198}$, but with much larger uncertainties (Table 1, see the Supporting Information).

It is generally accepted that since bacterial metabolism slows down at lower temperatures (*16*), preference for the lighter isotope and the extent of fractionation should increase. Moreoever, MerA is a thermophilic enzyme (*29*) and the lowered activity of MerA at low temperatures could potentially introduce another rate-limiting step (in addition to the Hg(II) uptake step) in the processing of Hg(II) by Hg(II) reducing bacteria. Possibly, the absence of a significant increase in fractionation (and alpha values) at lower temperatures is due to the increased fractionation by MerA, balanced by an equal decrease in fractionation during the uptake/transport steps. A similar rationale has been accepted as the reason for lack of any change in sulfur fractionation when a naturally occurring SRB community growing with lactate as an electron donor experienced change in incubation temperatures from 25 to 5 °C (*27*). Low temperatures decrease the fluidity of the membrane (*27*) and could limit the Hg(II) exchange reactions

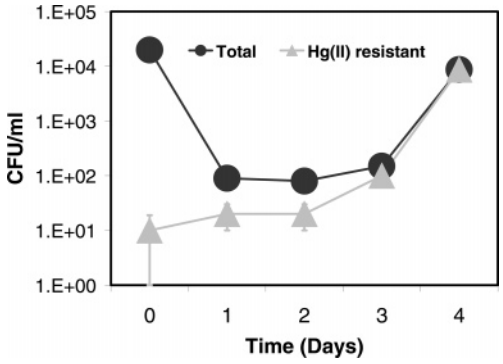

FIGURE 3. Enrichment of Hg^R microbes in a freshwater natural microbial consortium. Numbers of total heterotrophic Colony forming units (CFU)/mL and Hg^R CFU/mL in natural microbial community during pre-exposure are shown. Errors represent 2SD.

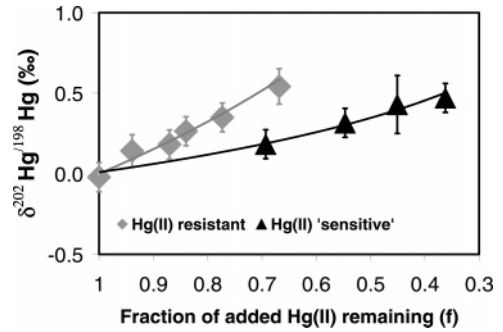

FIGURE 4. Measured δ^{202}Hg vs f for the reactor samples from the experiments with natural consortium enriched in Hg^R microbes and Hg^S natural community in site water containing 225 ng/g and 25 ng/g Hg(II), respectively. Curves correspond to $\alpha_{202/198} = 1.0013$ and 1.0004 for Hg^R and Hg^S communities, respectively. Error bars represent external precision as for Figure 1.

occurring within the outer membrane and/or transport across the inner membrane of the gram negative cell, thereby decreasing the fractionation during the Hg(II) uptake step.

Fractionation of Hg by Hg^R and Hg^S Natural Microbial Communities. To expand our observations on the isotopic fractionation of Hg(II) during its biological reduction from pure bacterial cultures to the activities of natural microorganisms in situ, we obtained a natural microbial community from a freshwater pond and enriched the indigenous Hg^R bacteria by pre-exposure to 225 ng/g Hg(II) (see Materials and Methods). During this pre-exposure period, the majority of Hg^S microorganisms died while the Hg^R microbes increased in biomass; at the end of the pre-exposure period all culturable surviving cells were Hg^R (Figure 3) and very likely carried and expressed *mer* operons (*21*). We did not supplement the site water with nutrients at any stage of this experiment but it is possible that the death of Hg^S microbes resulted in the release of significant amounts of organic electron donors available for use by the Hg^R microbes during pre-exposure (*21*). Since the enriched cells were harvested by centrifugation before resuspension in filter sterilized site water, excess electron donors were not carried over from the pre-exposure period.

When the resuspended enriched cells volatilized Hg from site water containing 225 ng/g NIST 3133 Hg(II), the δ^{202}Hg of the Hg(II) remaining in the reactor followed Rayleigh fractionation with $\alpha_{202/198}$ value (1.0013 ± 0.0004), within the range of alpha values for the pure culture experiments (Figures 4 and S4, Tables 1 and S4). We expected to observe more noise in this data because, even though all the microbes in the "adapted" natural microbial consortium are Hg^R, they must belong to diverse lineages, have differing metabolic potentials, and the microbial community composition can change during the length of the experiment (60 h).

To compare the extent of Hg fractionation by a Hg^R microbial consortium with a natural Hg^S community, microorganisms from the same water source were exposed to 25 ng/g Hg(II) (NIST 3133) without preceding pre-exposure. This lower level of Hg(II) exposure for the unadapted community, as compared to the adapted Hg^R consortium, was necessitated by the Hg(II) sensitivity of unadapted microbes such that higher levels of Hg(II) in the reactor would have resulted in cell death. In this cell suspension less than 10% of the colony forming units (CFU) were Hg^R. During the length of the experiment, the unadapted Hg^S community reduced 0.16 pg/g Hg(II) per CFU, in contrast to the Hg adapted consortium that reduced a 1000-fold more Hg(II) (0.162 ng/g per CFU). Reduction by the unadapted community resulted in a very small Rayleigh fractionation with $\alpha_{202/198} = 1.0004 \pm 0.0002$ (Tables 1 and S4).

A very low extent of Hg(II) loss during dark abiotic control experiments consisting of filtered water from the same site (<2% of the added Hg(II) volatilized) indicated that the loss of Hg(II) from the reactor in the experiment with the unadapted Hg^S community was due primarily to biological activity and not abiotic processes. The small amount of Hg reduced in the dark abiotic control experiments along with the smaller isotopic fractionation observed for the un-adapted community, suggests that dark biological reduction mechanisms, likely unrelated to MerA activities, do not cause significant Hg stable isotope fractionation. These mechanisms possibly include Hg(II) reduction by Hg^S microbes and/or their metabolic products (*2*). It is also possible that the reduced extent of fractionation by Hg^S community is partially due to suppression of fractionation at lower Hg(II) concentrations.

Implications and Future of Hg Isotope Systematics. Mercury resistant bacteria preferentially reduced lighter isotopes of Hg as expected from past studies on microbial fractionation of traditional (*3*) and non-traditional stable isotopes (*4*). The total range of δ^{202}Hg observed in the Hg transformations examined in this study is ~6‰ (Table S1) and is similar to the maximum fractionation per atomic mass unit (Table S5) observed for fractionation of much lighter elements including Fe and Mo (*4*). As pointed out by Smith et al. (2005) (Figure 4 in ref *8*), this large range of isotopic fractionation (i.e., δ^{202}Hg) of these heavy elements, including Hg, may be due to predominance of kinetic effects and redox sensitivity. A slightly smaller range of δ^{202}Hg (~5‰) was observed in hydrothermal ores (*8*) and sediments (*10*). Although Smith et al. (2004) suggested that high temperature inorganic mechanisms may be responsible for Hg isotope fractionation in hydrothermal ores (*8*), the present study suggests that MerA-expressing Hg^R thermophillic bacteria (*29*) could also contribute to the isotopic fractionation observed in hydrothermal deposits.

The overlapping range of $\alpha_{202/198}$ values (best estimates from each experiment ranging from 1.0013 to 1.0020) observed for one Hg^R pure culture as well as a natural consortium of Hg^R microbes, and the non-dependence of the fractionation factor on growth temperature, imply that bacterial Hg(II) uptake and reduction via the ubiquitous and efficient *mer* pathway could yield a consistent isotopic signature under differing experimental conditions. The progressive suppression in Hg(II) fractionation observed when the Hg(II) concentration in the reactor falls below ~180 ng/g in both 1 L experiments done at 37 °C (Table S1) is interesting. In naturally occurring aquatic environments, the Hg(II) concentrations are lower than 180 ng/g but since the induction of *mer* operon is quantitatively related to the concentration of bioavailable Hg(II) (*15*), the molar ratio of reactant Hg(II) to Mer proteins, including MerA, will not

become as low as it possibly became during our experiments. Therefore, the environmental relevance of this decrease in the extent of fractionation at lower concentrations of Hg(II) could depend on a variety of factors that must be explored in future studies. It is highly probable that even though we found a narrow range of alpha values at differing temperatures for one exponentially growing gram negative pure culture of bacteria grown with abundant electron donor and high Hg(II) concentrations, other growth conditions and/or other Hg^R bacterial species will not lead to similar extent of Hg fractionation because of differences in number and kind of rate-limiting steps in the reduction pathway.

We also note that our experiments were carried out using ng/g levels of Hg while in most natural waters, where the accumulation of MeHg in biota is of public health concern, Hg concentrations are often in the sub-ng/g range. Currently our analysis is limited by the size of our reactor and the sensitivity of high-precision MC-ICPMS measurements. Future analytical developments are likely to enable determination of Hg stable isotope ratios in experimental products with lower concentrations of Hg.

This study, along with additional studies of similar and other Hg redox transformations, could give insights into Hg accumulation in natural sediment samples which typically contain abundant Hg (high ng/g levels) and are easily measured archives of the Hg isotopic composition of aquatic systems (*9*−*10*). We expect that further experimentation will reveal multiple mechanisms leading to Hg isotope fractionation, but nevertheless, it seems likely that isotopic measurements will prove helpful in tracking changes in the redox state of Hg in aquatic and terrestrial environments in a manner analogous to the isotope systematics of other heavy elements such as Cr (*5*) and Fe (*6*).

In summary, we have provided clear evidence of systematic mass dependent kinetic fractionation of Hg isotopes. Hg is one of the heaviest elements for which significant biological fractionation has been observed, and our work adds to the growing number of heavy elements for which stable isotope systematics has been successfully developed in the past decade (*4*). Our work suggests that Hg isotopes might have the potential for distinguishing between different sources of Hg(0) emissions based on the extent of Hg isotope fractionation. Thus, this work is an important initial step in the development of Hg isotope systematics for the purpose of identifying Hg sources and sinks in the environment, for determining in situ pathways affecting Hg toxicity, and for investigating the nature and evolution of Hg redox reactions in both modern and paleo environments.

Acknowledgments

We are grateful for the in-depth suggestions by three anonymous reviewers which have greatly improved this manuscript. We acknowledge M. Meredith for help with experiments at Rutgers and helpful comments by Drs. B. Klaue, J. Reinfelder, and P. Falkowski. Funding was provided by the NSF (EAR-0433793 to T.B. and EAR-0433772 to J.D.B.) and a Graduate Student Award to K.K. by the New Jersey Water Research Resource Institute.

Supporting Information Available

Additional text, stable isotopic data, and Rayleigh plots from all experiments. This material is available free of charge via the Internet at http://pubs.acs.org.

Literature Cited

(1) Fitzgerald, W. F.; Mason, R. P.; Vandal, G. M. Atmospheric cycling and air-water exchange of Hg over mid-continental lacustrine regions. *Water Air Soil Pollut.* **1991**, *56*, 745−767.

(2) Barkay, T.; Wagner-Döbler, I. Microbial transformations of mercury: potentials, challenges, and achievements in controlling mercury toxicity in the environment. *Adv. Appl. Microbiol.* **2005**, *57*, 1−52.

(3) Valley, J. W.; Cole, D. R. *Stable Isotope Geochemistry*; The Mineralogical Society of America: Washington, DC, 2001; Vol. 43.

(4) Johnson, C. M.; Beard, B. L.; Albarède, F. *Geochemistry of Non-Traditional Stable Isotopes*; The Mineralogical Society of America: Washington, 2004; Vol. 55.

(5) Johnson, T. M.; Bullen, T. D. In *Geochemistry of Non-Traditional Stable Isotopes*; Johnson, C. M., Beard, B. L., Albarede, F. Eds.; The Mineralogical Society of America: Washington, DC, 2004; Vol. 55.

(6) Johnson, C. M.; Beard, B. L.; Roden, E. E.; Newman, D. K.; Nealson, K. H. In *Geochemistry of Non-Traditional Stable Isotopes*; Johnson, C. M., Beard, B. L., Albarede, F., Eds.; The Mineralogical Society of America: Washington, DC, 2004; Vol. 55.

(7) Hintelmann, H.; Lu, S. Y. High precision isotope ratio measurements of mercury isotopes in cinnabar ores using multi-collector inductively coupled plasma mass spectrometry. *Analyst* **2003**, *128*, 635−639.

(8) Smith, C. N.; Kesler, S. E.; Klaue, B.; Blum, J. D. Mercury isotope fractionation in fossil hydrothermal systems. *Geology* **2005**, *33* (10), 825−828.

(9) Jackson, T. A.; Muir, D. C.; Vincent, W. F. Historical variations in the stable isotope composition of mercury in Arctic lake sediments. *Environ. Sci. Technol.* **2004**, *38* (10), 2813−2821.

(10) Foucher, D.; Hintelmann, H. High-precision measurement of mercury isotope ratios in sediments using cold-vapor generation multi-collector inductively coupled plasma mass spectrometry. *Anal. Bioanal. Chem.* **2006**, *384* (7−8), 1470−1478.

(11) Blum, J. D. unpublished data.

(12) Mason, R. P.; Fitzgerald, W. F.; Morel, F. M. M. Aquatic biogeochemical cycling of elemental mercury: anthropogenic influence. *Geochim. Cosmochim. Acta.* **1994**, *58*, 3191−3198.

(13) Fitzgerald, W. F.; Mason, R. P.; Vandal, G. M.; Dulac, F. In *Mercury as a Global Pollutant: Toward Integration and Synthesis*; Watras, C. J., Huckabee, J. W., Eds.; Lewis Press: Boca Raton, FL, 1994; pp 203−220.

(14) Schaefer, J. K.; Yagi, J.; Reinfelder, J.; Cardona-Marek, T.; Ellickson, K.; Tel-Or, S.; Barkay, T. The role of the bacterial organomercury lyase (MerB) in controlling methylmercury accumulation in mercury contaminated natural waters. *Environ. Sci. Technol.* **2004**, *38*, 4304−4311.

(15) Barkay, T.; Miller, S. M.; Summers, A. O. Bacterial mercury resistance from atoms to ecosystems. *FEMS Microbiol. Rev.* **2003**, *27*, 355−384.

(16) Canfield, D. E. In *Stable Isotope Geochemistry*; Valley, J. W., Cole, D. R., Eds.; The Mineralogical Society of America: Washington, DC, 2001; Vol. 43.

(17) Hoefs, J. *Stable Isotope Geochemistry*. 4th ed.; Springer-Verlag: Berlin Heidelberg, 2004.

(18) Reniero, D.; Galli, E.; Barbieri, P. Cloning and comparison of mercury- and organomercurial-resistance determinants from a Pseudomonas stutzeri plasmid. *Gene* **1995**, *166* (1), 77−82.

(19) Sambrook, J.; Fritsch, E. F.; Maniatis, T. Molecular Cloning: A Laboratory Manual; Cold Spring Harbor Laboratory Press: New York, 1989; Vol. 3.

(20) Selifonova, O.; Burlage, R.; Barkay, T. Bioluminescent sensors for detection of bioavailable Hg(II) in the environment. *Appl. Environ. Microbiol.* **1993**, *59* (9), 3083−3090.

(21) Barkay, T. Adaptation of aquatic microbial communities to Hg^{2+} stress. *Appl. Environ. Microbiol.* **1987**, *53*, 2725−2732.

(22) Bergquist, B. A.; Blum, J. D. Abiotic fractionation of mercury stable isotopes. in preparation.

(23) Lauretta, D. S.; Klaue, B.; Blum, J. D.; Buseck, P. R. Mercury abundances and isotopic compositions in the Murchison (CM) and Allende (CV) carbonaceous chondrites. *Geochim. Cosmochim. Acta* **2001**, *65*, 2807−2818.

(24) Scott, K. M.; Lu, X.; Cavanaugh, C. M.; Lu, J. S. Optimal methods for estimating kinetic isotope effects from different forms of the Raleigh distillation equation. *Geochim. Cosmochim. Acta* **2004**, *68*, 433−442.

(25) York, D. Least-squares fitting of a straight line. *Can. J. Phys.* **1966**, *44*, 1076−1086.

(26) Wilson, J. R.; Leang, C.; Morby, A. P.; Hobman, J. L.; Brown, N. L. MerF is a mercury transport protein: Different structures but a common mechanism for mercuric ion transporters? *FEBS Letters* **2000**, *472* (1), 78−82.
(27) Canfield, D. E. Isotope fractionation by natural populations of sulfate-reducing bacteria. *Geochim. Cosmochim. Acta* **2001**, *65* (7), 1117-1124.
(28) Barkay, T.; Gillman, M.; Turner, R. R. Effects of dissolved organic carbon and salinity on bioavailability of mercury. *Appl. Environ. Microbiol.* **1997**, *63* (11), 4267−4271.
(29) Vetriani, C.; Chew, Y. S.; Miller, S. M.; Yagi, J.; Coombs, J.; Lutz, R. A.; Barkay, T. Mercury adaptation among bacteria from a deep-sea hydrothermal vent. *Appl. Environ. Microbiol.* **2005**, *71* (1), 220−226.

Received for review August 22, 2006. Revised manuscript received December 20, 2006. Accepted December 21, 2006.

ES062019T